



جامعة أبو بكر بلقايد-
تلمسان

University of Abou Bakr Belkaïd Tlemcen

Faculty of Technology

Biomedical engineering department

Biomedical Engineering research laboratory

Thesis project

To obtain :

A MASTER degree in Biomedical Engineering

Specialty :

Biomedical Instrumentation

Presented by :

Hadjersi Anes

**A TEST bench to measure microfluidic flow-rates
of microvalves**

Presenting on 4th of July, in front of the juries:

Mr	Kerai Salim	<i>MCA</i>	University of Tlemcen	President
Mm	Bendelhoum	<i>MCB</i>	University of Tlemcen	Examiner
Mr	Soulimane Sofiane	<i>MCA</i>	University of Tlemcen	supervisor

University year 2018-2019

Acknowledgement

In the name of ALLAH, the most gracious, the most merciful, we start this work. Here, it is five years of studying is about to finish. I have known so many people, I have learnt so many things during this incredible experience, there were moments of satisfaction and other bad moments of course, but in general it was quite good.

Firstly, I would like to thank ALLAH for every blessing who gave me during this work or during these five years of studying. A special thanks to my family, my father and mother who support me in each step that I make. A special thanks to my professors that I have met. Also, I would like to greet my professor and my supervisor Mr Soulimane Sofiane who helped me a lot during my project and who gave me this huge opportunity to discover the GBM Laboratory team work. Without forgetting my co-supervisor Mr Slami Ahmed, who taught me so many professional things.

Thank you so much dearest people and thank ALLAH for knowing such people.

Table of materials

Abstract.....	7
---------------	---

Chapter 1. Generalities and state of art.

I. Introduction	1
II. Measurement methods	1
II.1. Measurements by heat exchange	1
II.2. Measurements by weighing the liquid	2
II.3. Measurements by noting the variation of pressure	2
II.4. Measurements by displacement of a meniscus	3
III. Fluidic laws	4
IV. Methodology.....	6
V. Conclusion.....	7

chapter2. The syringe driver and calibration.

I. Introduction	9
II. The Microcontroller Arduino board	9
III. Arduino motor shield Rev3	10
IV. The hardware parts.	11
V. Stepper motor pm551-048-hp69.....	12
VI. Calibration of the syringe-driver.	13
VII. LCD display and Keypad.	14
VIII. Test bed with an Optical mounting.....	15
1. The flow-rate measurement.	15
2. The flow-rate calibration.	18
IX. Conclusion.....	19

Chapter3. flow-rates measurements in valves micro-pumps.

I. Introduction.	20
II. Diffuser/ nozzle structure	20
III. Enhanced diffuser/nozzle structure.....	21
IV. Microfluidic structure realization	21
IV.2. Masters of molds fabrication	22
IV.3 Test protocol of micro-valves.....	23

V. Conclusion.....	24
References	26

Figure table

Chapter 1.

Fig 1. Measurements by heat exchange.

Fig 2. Flow meter by weighing the liquid Schnell (1997).

Fig 3. Measurements by noting the variation of pressure.

Fig 4. Measuring the flow by the meniscus moving Urbanek *et al.*

Fig 5. Ranges of use of various test benches for the measurement of micro-flow.

Fig 6. Venturi effect.

Fig 7. Poiseuille's Law.

Fig 8. MIRE ruler.

Fig 9. The design of the differential pressure sensor.

Chapter 2.

Fig 10. 24PCFA6D unamplified differential pressure sensor.

Fig 11. Arduino MEGA and Arduino UNO.

Fig 12. Arduino motor shield Rev3.

Fig 13. The pins breakdown.

Fig 14. The 3D printer design..

Fig 17. LCD display pins.

Fig 19. Keypad connections.

Fig 20. Final syringe driver

Fig 21. The digital microscope.

Fig 22. The fluid's displacement under microscope.

Fig 23. Pixel/mm conversion.

Fig 24. The Flow-rate equation.

Fig 25. The test-bed interface.

Fig 26. The linear fit flow-rate/Time.

Chapter 3.

Fig 27. The design of the micro-pump.

Fig 28. Diffuser/nozzle structure.

Fig 29. The design of the air diffuser/nozzle.

Fig 30. The negative mold of air diffuser/nozzle structure.

Fig 31. The 3D printed ABS structures.

Fig 32. Micro-pump mechanism.

Fig 33. Testing the simple diffuser/nozzle structure.

Table list

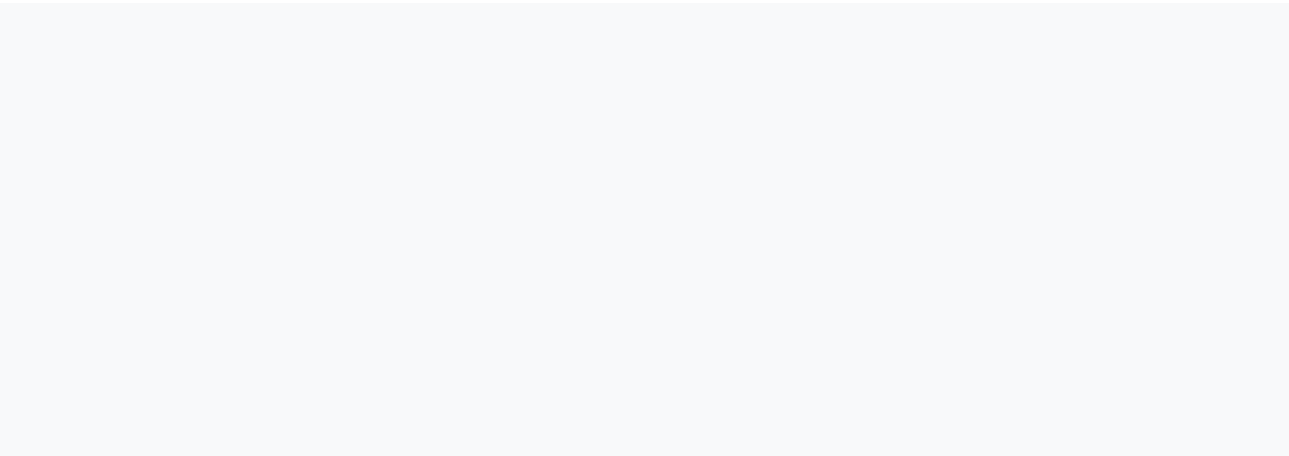
Tab1. The metal mechanical parts.

Tab2. The motor data sheet.

Tab3. LCD display pin's signification.

Tab4. The experimental measurements.

Tab5. The result table.



ملخص

يتعلق هذا المشروع بالتحليل التجريبي لأنظمة مايكروسيستم السائلة ، وكذلك تحسين الدوائر الصغيرة فلويديك. ينصب التركيز الرئيسي لعملنا على تصميم وبناء وتشغيل قاعدة اختبار محددة. يتم استخدام مقعد الاختبار هذا بشكل خاص لدراسة اختبار أنواع مختلفة من الصمامات مثل بنية الناشر / الفوهة. سيتم تثبيت هذه الهياكل على مضخة صغيرة لحقن المخدرات على سبيل المثال. عملنا هو تحقيق طاولة اختبار لقياس معدل التدفق السائل لأننا نعرف أن قياس التدفق له أهمية Poiseuille وكذلك الضغط المرتبط باستخدام قانون أساسية في شبكات نقل السوائل. تكون ظروف الضغط ودرجة الحرارة عموماً بنفس الترتيب الذي تم قياسه للأنظمة العيانية. يرتبط تصميم نظامنا بتدفق السائل في القناة الصغيرة. أظهرت نتائجنا دقة قياس معدل التدفق لحوالي اللتر الصغرى بالدقيقة "ميكرو لتر / دقيقة". الناشر / فوهة مع تحكم عالية الدقة لقياس microvalves تُستخدم هذه الطريقة لاختبار بنية التدفق الصغير والتدفق. من منظورنا، تسمح لنا طاولة الاختبار باختبار أنواع مختلفة من المضخات الصغيرة و / أو الصمامات الدقيقة للتسليم الدوائي السريع المصمم في مختبر الهندسة الطبية الحيوية.

Abstract

This project concerns the experimental analysis of liquid fluidic Microsystems, as well as the optimization of micro-fluidic circuit. The main focus of our work is to design, build and operate a specific test bench. This test bench is used particularly for the study of testing different valves like the diffuser/nozzle structure. These structures will be installed on a micro-pump for drug injection for instance. Our work is the realization of a test bench for measuring the fluidic flow rate as well as the relating pressure by using the Poiseuille's law because as we know that the flow measurement has a fundamental importance in the fluid transport networks. The pressure and temperature conditions are generally in the same order as those measured for macroscopic systems. The design of our system is related to flow of liquid in the micro-channel. Our results showed a measurement precision of flow-rate for about the micro-liter by minute " $\mu\text{l}/\text{min}$ ". This method is used to test diffuser/nozzle microvalves structure with high precision control of the micro-flow and flowrate measurement. In perspective, our test bench allows us to test different kinds of micro-pump and/or micro-valves for rapid drug delivery designed in Biomedical Engineering laboratory.

Résumé

Ce projet concerne l'analyse expérimentale de microsystèmes fluidiques liquides, ainsi que l'optimisation de circuits micro-fluidiques. L'objectif principal de notre travail est de concevoir, de construire et d'exploiter un banc d'essai spécifique. Ce banc d'essai est particulièrement utilisé pour l'étude de différents types de vannes comme la structure diffuseur/ nozzel (buse). Ces structures seront installées sur une micro-pompe pour l'injection de médicaments, par exemple. Notre travail consiste à réaliser un banc d'essai permettant de mesurer le débit de fluide ainsi que la pression correspondante en utilisant la loi de Poiseuille, car nous savons que la mesure de débit a une importance fondamentale dans les réseaux de transport de fluide. Les conditions de pression et de température sont généralement dans le même ordre que celles mesurées pour les systèmes macroscopiques. La conception de notre système est liée à l'écoulement de liquide dans le micro-canal. Nos résultats ont montré une précision de mesure du débit pour environ le micro-litre par minute « $\mu\text{l}/\text{min}$ ». Cette méthode est utilisée pour tester la structure des microvalves de diffuseur/nozzel avec un contrôle de haute précision du micro-débit et de la mesure du débit. En perspective, notre banc d'essai nous permet de tester différents types de micro-pompes et / ou de micro-valves pour l'administration rapide de médicaments conçus dans le laboratoire de génie biomédical.

Introduction.

Microsystems are composed of various elements interacting with each other and operating in a specific domain. We can find plenty of Microsystems types depending on the domain of application, such as optical, mechanicals, fluidics... These elements have the function of micro-sensors or micro-actuators. To be called microsystem, one of the three dimensions of the systems must be from micrometer to millimeter.

In our project, we will be interested on the micro-fluidic devices. We call a fluidic Microsystem each system using or carrying: liquid or gas, mono or multiphase fluids. They have grown considerably in recent years, thus we can find for instance: lab on chip "LOC", as well as, biomedical implantable devices in the human body. Another type of fluidic Microsystem is drug delivery using micro-pumps which are divided on two groups. We can find slow drugs infusing about one micro-liter by minute ($\mu\text{l}/\text{min}$) and rapid injection about one milliliter by second (ml/s) [1]. We can find also a large pressure and flow-rate intervals. Depending on these two categories, we define the flow measurement range according to the miniaturization used.

Our work will be focused on testing the micro-pumps realized by researchers at GBM laboratory. Where, they are working on insulin injection by a miniaturized connected patch applied to diabetic patients and vacuum micro-pumping for smart Band-Aid.

For micro-pumps characterization, we must take in consideration the following points: the reliability of the sensor which is very important, as well as, the reproducibility which means having the same result for each measurement or test.

We hope to design a test bench to measure fluidic pressure and flow-rate of the above micro-pumps. Several physical characteristics such as : pressure, mass, volume-flow, or temperature of the test element or fluid, must be measured accurately. This allows to validate or to detect the possible defects relating to the technological choices and the miniaturization techniques that need to be corrected.

This report is organized as following:

- First of all, in the chapter 1, we expose some generalities and state of art in which we are aiming to identify some methods used to determine the flow-rate as well as some equations and Laws related to micro-fluidic domain.
- Then, in chapter 2, we are detailing the syringe driver realization and its mechanism calibration as well as the flow-rate measurement calibration.
- Afterwards, in chapter3, we expose the structures that we hope realizing, the PDMS preparation and then the testing and the results that we have obtained.
- Finally, it will have a general conclusion and perspectives.

Chapter 1.

Generalities and state of art

I. Introduction

For the measurement of the micro-flow, several techniques are used, each one has a specific characteristics in terms of the measuring range, calibration with the weak levels (that is often hard), and of course the realization cost in terms of the components that are used.

In this section, we are going to talk about these principles and the reason of choosing measuring the flow by the meniscus moving, this measurement is simple to be realized at the macroscopic scale, since there are a large number of mass or volume flow-meters.

In addition of that, to obtain an accurate measurement, an optical microscope is used to detect the passage of the meniscus. We can find four techniques described in following paragraphs [2].

- Measurements by heat exchange.
- Measurements by weighing the liquid.
- Measurements by noting the variation of pressure.
- Measurements by displacement of a meniscus.

II. Measurement methods

Here, we discuss the principle of each method.

II.1. Measurements by heat exchange

For this measurement, we put in a flow a heater resistance, based on the Joule effect at a temperature higher than the temperature of this flow; a convective heat exchange is generated. This exchange is a function of the physical properties of the fluid. It is thus possible to access the speed or volume flow by analyzing the heat transfer Q (principle of thermal anemometry).

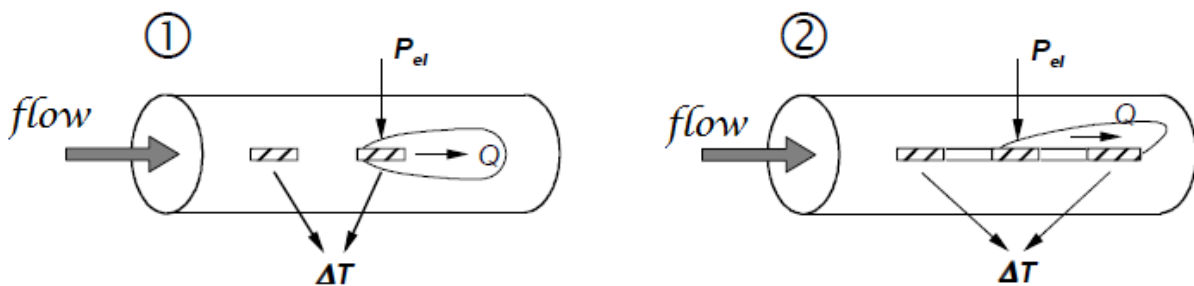


Fig 1. Measurements by heat exchange.

Different types of the sensor configurations are utilized (Fig 1). The first (1) consists of a heating resistor and a thermistor, placed inside a pipe. The velocity of the fluid is calculated from the electric puissance P_{el} required to maintain the resistance at a constant temperature. The second type of sensor (2) consists of a heating resistor placed between two thermistors. The fluid is heated through the resistance. The flow rate is then calculated from the temperature measurement upstream and downstream of the hot point. It is necessary to design thin thermistors in order to not disturb the flow.

II.2. Measurements by weighing the liquid

Richter et al. [3] uses a precision balance to determine the mass of a volume of liquid in a tank in function of time. The measurement accuracy depends directly on the accuracy of the scale. The measuring range is from 1 to 1000 $\mu\text{l}\cdot\text{min}^{-1}$. Schnell [4] developed an original system (Fig 2) using an optical sensor (2) to access the mass of a drop of liquid exiting the tip of the test tube. The sensor detects bending of the tube created by the formation of the drop. The set is placed in a chamber (1) to avoid any external disturbance. The flow rates thus obtained are in a range from 10 to 1600 $\mu\text{l}\cdot\text{min}^{-1}$, the calibration having been carried out using a Mettler PM 100 precision balance.

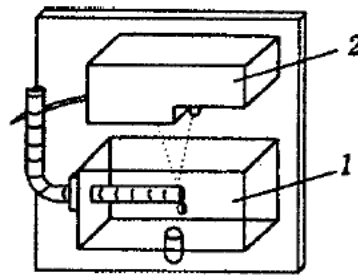


Fig 2. Flow meter by weighing the liquid Schnell (1997) [2].

In this system, we must take in consideration the following points:

- The system must be perfectly configured horizontally in order to get an identical formation of the drop for all measurements.
- The choice of the tube material is essential.
- The sensor used has an accuracy of 0.5 μm .

The authors denote that this system is unfortunately very sensitive to vibrations.

II.3. Measurements by noting the variation of pressure

This system, developed by Schnell [5], measures a static pressure variation in a tank over time, converted into a volume change (a). In order to eliminate the influence of certain parameters (notably the temperature of the liquid) and increasing the sensitivity of the measuring system, the volume is obtained by differential pressure measurement in two tubes connected to each other. This configuration also allows realizing a pendulum system, to rebalance the pressures for a next measurement (b).

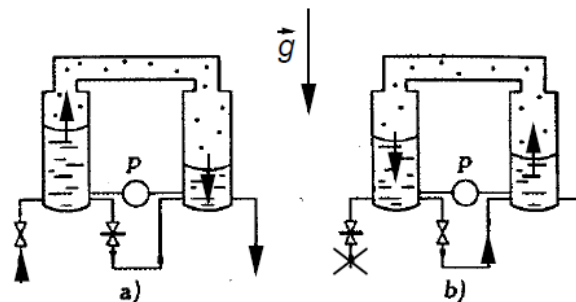


Fig 3. Measurements by noting the variation of pressure [5].

This system allows the measurement of flow rates between 10 and $2000 \mu\text{l min}^{-1}$, the Microsystems can be connected upstream or downstream of the measurement system. However, it can only work in a vertical position.

II.4. Measurements by displacement of a meniscus

The volume flow is in this case obtained by measuring the velocity of the liquid in a capillary calibrated by the MIRE RULER. This speed is calculated by knowing the time t that will put this liquid to travel a distance d . The accuracy of the measurement depends on the syringe volume calibration and the distance measurement errors. In order to reduce these measurement uncertainties, an optical microscope is used to monitor the progress of the liquid. From the knowledge of the speed and the section of the capillary, it is then easy to determine the flow rate. This system allows a wide range of measurement, adapting the volume of the syringe to the flow rates to be measured.

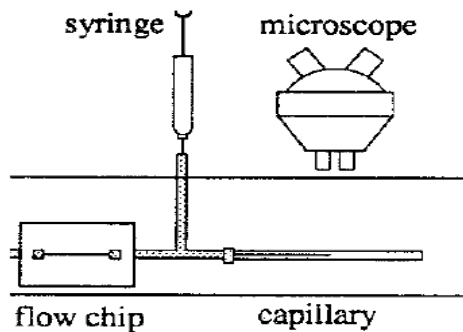


Fig 4. Measuring the flow by the meniscus moving Urbanek *et al.* [3].

The figure 5 describes the range of using a various test benches for the micro-flow measurement. Where, a polyvalent test bench can be achieved to test any fluidic Microsystem. It is important to be able to cover a wide range of flow rates (typically between 10^{-13} to $10^{-7} \text{m}^3\text{s}^{-1}$).

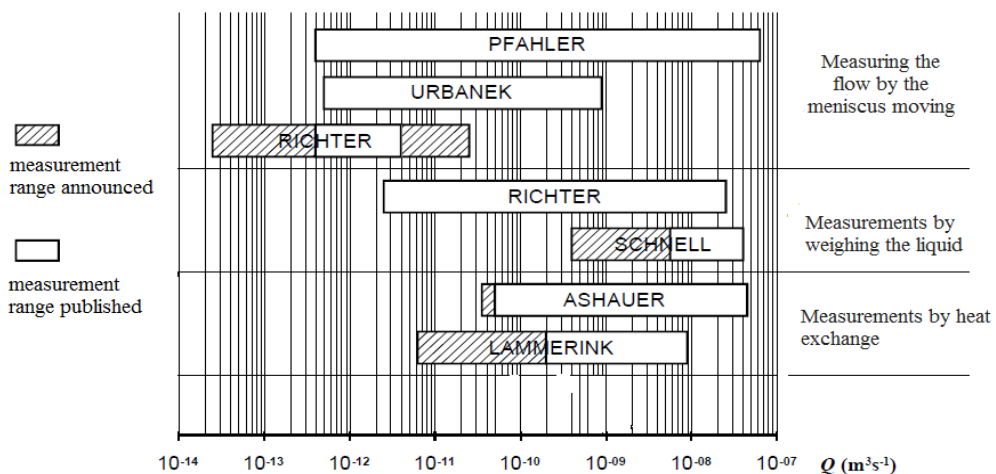


Fig 5. Ranges of use of various test benches for the measurement of micro-flow [6].

In this project, we have developed this method to measure fluid flows in microfluidic structures. This choice is due to the availability of components and the reliability of this method.

II. Fluidic laws

Several equations exist while a fluid is displacing, depending on the section of the tube in which the fluid circulates, the molecular properties of the fluid substance, the velocity... and other parameters.

Here, we are going to expose fundamental equations of fluids also used in microfluidic technologies.

1. Venturi effect

When flowing through a constricted area of a pipe, a fluid's velocity increases and its static pressure decreases. This principle is known as the Venturi effect. The effect based on the principle of continuity as well as the principle of conservation of mechanical energy.

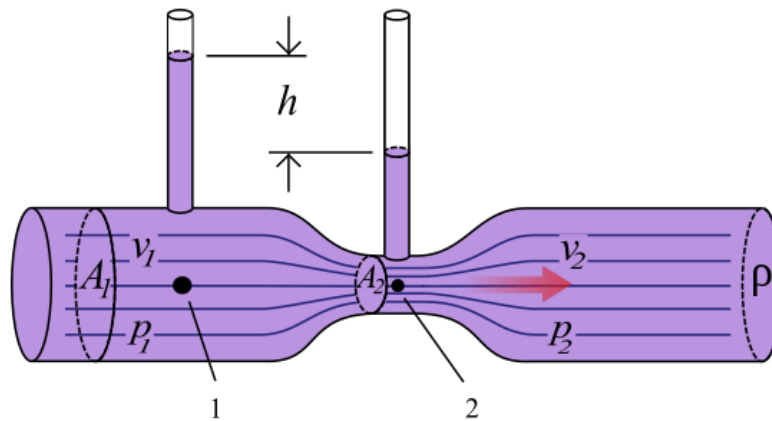


Fig 6. Venturi effect.

The static pressure in the first measuring tube (1) is higher than at the second (2), and the fluid speed at “1” is lower than at “2”, because the cross-sectional area at “1” is greater than at “2”. By measuring the change in pressure, the flow rate can be determined by using a Venturi tube. The device is used in several industrial applications because it is the simplest and most accurate form of volume flow rate measurement. Manometers or transducers are installed on the two different sections (“free flow” and small”) to measure the pressure difference, as shown in the picture above. Since we know the geometry of the Venturi meter (A_1 , A_2), and the fluid characteristics (viscosity and density), the flow rate can be easily calculated via:

$$Q = A_1 \cdot \sqrt{\frac{2}{\rho} \cdot \frac{p_1 - p_2}{\left(\frac{A_1}{A_2}\right)^2 - 1}} = A_2 \cdot \sqrt{\frac{2}{\rho} \cdot \frac{p_1 - p_2}{1 - \left(\frac{A_2}{A_1}\right)^2}} \quad \dots(1)$$

2. Bernoulli equation.

In fluid dynamics, Bernoulli's principle states that an increase in the speed of a fluid occurs simultaneously with a decrease in pressure or a decrease in the fluid's potential energy.

Bernoulli's principle can be applied to various types of fluid flow, resulting in various forms of Bernoulli's equation; there are different forms of Bernoulli's equation for different types of flow. The simple form of Bernoulli's equation is valid for incompressible flows (e.g. most liquid flows and gases moving at low Mach number). More advanced forms may be applied to compressible flows at higher Mach numbers.

Chapter 1. Generalities and state of art.

In most flows of liquids, and of gases at low Mach number, the density of a fluid parcel can be considered to be constant, regardless of pressure variations in the flow. Therefore, the fluid can be considered to be incompressible and these flows are called incompressible flows.

$$\frac{v^2}{2} + g \cdot z + \frac{p}{\rho} = \text{constant} \dots(2)$$

Where :

- v is the fluid flow speed at a point on a streamline.
- g is the acceleration due to gravity.
- z is the elevation of the point above a reference plane.
- p is the pressure at the chosen point.
- ρ is the density of the fluid at all points in the fluid.

By applying this equation in two different points we can find:

$$p_1 - p_2 = \frac{\rho}{2} (V_1^2 - V_2^2) \dots(3)$$

3. Poiseuille Law.

Poiseuille equation, is a physical law that gives the pressure drop in an incompressible and Newtonian fluid in laminar flow flowing through a long cylindrical pipe that is substantially longer than its constant diameter; and there is no acceleration of fluid in the pipe.

In standard fluid-kinetics notation:

$$\Delta p = \frac{8 \mu L Q}{\pi R^4} \dots(4)$$

- ΔP is the pressure difference between the two ends,
- L is the length of pipe,
- μ or η is the dynamic viscosity,
- Q is the volumetric flow rate,
- R or r is the pipe radius.

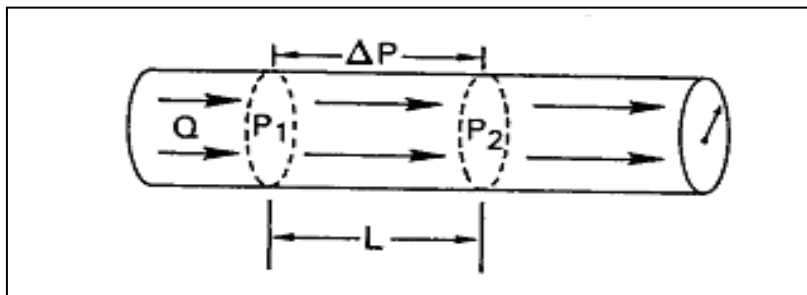


Fig7. Poiseuille's Law principle.

Our project will be realizing a test bench in order to measure the generated pressure and the micro-flow of the micro-fluidic systems. We choose a concept based on the method of measuring the flow by the meniscus

Chapter 1. Generalities and state of art.

moving. Here, we will use the optical mounting, and if we can provide the differential pressure sensor we will use it to validate and verify the optical assembly. For this, we must manage the following actions:

- Fluid syringe or micro actuator force calibration,
- Pumping and capillary connector installation.
- Optical assembly.
- Testing the diffuser/nozzle structure.

At the end, we must measure the pressure and the flow rate of the micro pumps. The results can be compared to Finite elements modeling study used by Comsol multiphysics application.

III. Methodology

We planned our work in two methods:

1. The optical mounting.

We will use a microscope to visualize the lines of the fluid, and we can inject a fluorescent substance to follow the fluid course. In addition, we will use a MIRE RULER, it is a graduated ruler used to get a precise measurement of an object's size, and we will use the ruler and the color in order to know the exact displacement of the fluidic channel.

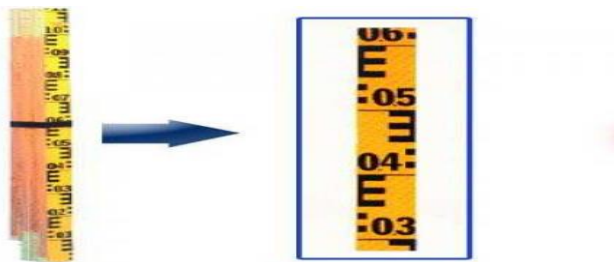


Fig 8. MIRE ruler.

By knowing the displacement and the time, we can conclude the speed of the fluid (velocity). As a result of that, we can know the flow rate because the section diameter is known.

2. Mounting with the differential pressure sensor.

We also hope using another mounting realized with a differential pressure sensor; we will order this kind of sensor. And we will try using it to verify the optical mounting and validating the results.

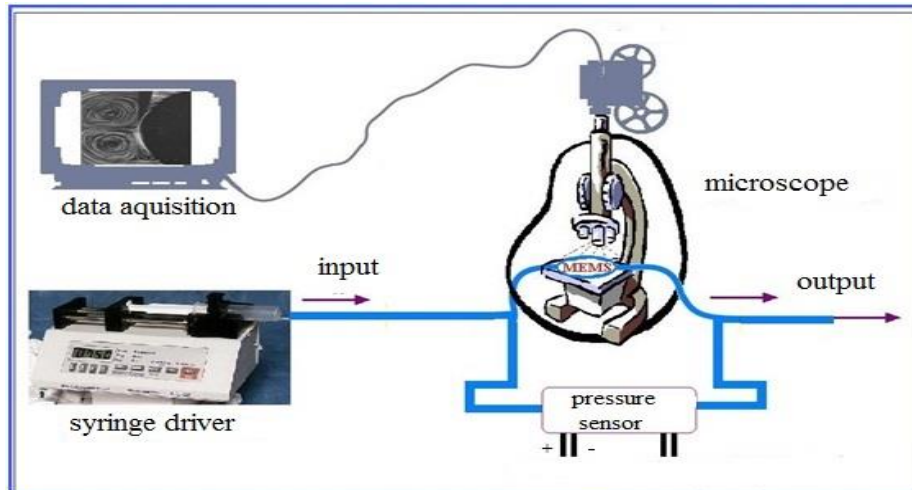


Fig 9. The design of the differential pressure sensor

This sensor is called Honeywell 24PC used for measuring miniature pressure ranges and in wet conditions. This kind of sensor is the right choice in our condition work. The concept is to measure the differential pressure of the input and output and afterwards we convert it to a flow-rate using Poiseuille Law.

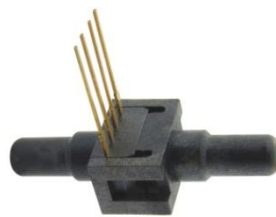


Fig 10. 24PCFA6D unamplified differential pressure sensor.

We have spent some many days dealing with this sensor using the right Arduino code. Honestly, we had some variations and unknown numbers. In this case, we must find a plan in order to calibrate the sensor. Unfortunately, the sensor was broken while we were calibrating. In addition, the mire ruler was not provided for the optical mounting so we had to find a solution for measuring the distance of the fluid, we will detail this method in the coming lines.

IV. Conclusion.

In this chapter, we outlined some methods used for measuring the flow-rate. Where, we choose measurements by displacement of a meniscus method to measure fluid flows in microfluidic structures. This choice is due to the availability of components and the reliability of this method. In addition, we focus about the equations and Laws existing in the fluidic and microfluidic field. In the coming chapters, we will details the used components and method of conception of a controlled syringe. Also, we will details the flow-rate measurement in a micro-channel based on Poiseuille's law by focusing on the optical microscope.

Chapter 2.

The syringe driver realization and their calibration

I. Introduction

This chapter describes the syringe pump realization, covering its design and function part by part, with the description of the hardware and software. Our aim is to realize a syringe driver in order to simulate the functionality of the miniaturized micro-pump. Our syringe pump is intended mainly for the usage in experimental Micro-fluidics, therefore it is more important how it performs with low volumes. The goal of the syringe driver is the ability of delivering a known volume in a continuous manner slowly. Therefore, this syringe pump will accurately control flow rates at different scales in different microfluidic structures. Firstly, we had the idea of using a useless DVD lecture that has the same mechanism that we wish realizing. The DVD lecture has two small stepper motors and one DC motor, the difficulty was how to calibrate these motors to make the motor pushing the volume slowly. We try the stepper motor ordered by an Arduino card, it has given us a satisfied result but when we fill the syringe with water, the motor cannot push the syringe unless we increase the motor's speed. Thus, we decided to use the DC motor with an appropriate Arduino code (more explanation below). Also, we used a 3D printer in order to create a support for the DVD lecture, the support form and shape was designed by Comsol Multiphysics, after a while time; the design was perfectly realized. Unfortunately, DC motor does not allow optimal control of the injection. As we know that the stepper motor is the right choice for this kind of projects, because it gives the opportunity to control the speed and to know the exact steps of the motor, for this purpose; we have decided to restart the project and create it from a to z. In the following paragraphs, we will describe the software and hardware parts used in the automatic syringe driver.

II. The Microcontroller Arduino board

Thanks to its simple and accessible user experience, Arduino has been used in thousands of different projects and applications. There are many other microcontrollers and microcontroller platforms available for physical computing, but the reasons of choosing Arduino are:

- Inexpensive : Arduino boards are relatively inexpensive compared to other microcontroller platforms. The least expensive version of the Arduino module can be easily assembled, and even the pre-assembled Arduino modules cost less than \$50
- Cross-platform : Arduino Software (IDE) runs on Windows, Macintosh OSX, and Linux operating systems. Most microcontroller systems are limited to Windows.
- Simple and clear programming environment : Arduino Software (IDE) is easy-to-use for beginners, yet flexible enough for advanced users to take advantage of as well.
- Open source and extensible software : Arduino software is published as open source tools, available for extension by experienced programmers. The language can be expanded through C++ libraries.

Arduino is an open-source electronics platform based on easy use of hardware and software. Arduino boards are able to read inputs and turn it into an output by telling your board what to do and sending a set of instructions to the microcontroller on the board. We must use the Arduino programming language (based on Wiring), and the Arduino Software (IDE), based on Processing. Many kinds of Arduino boards exist nowadays, the most known kinds are: Arduino UNO, Arduino DUEMILANOVE, Arduino DIECIMILA, Arduino NG REV.C, Arduino BT, Arduino MEGA ... The most used are Arduino UNO and Arduino MEGA. In our project, we worked with the Arduino MEGA board.

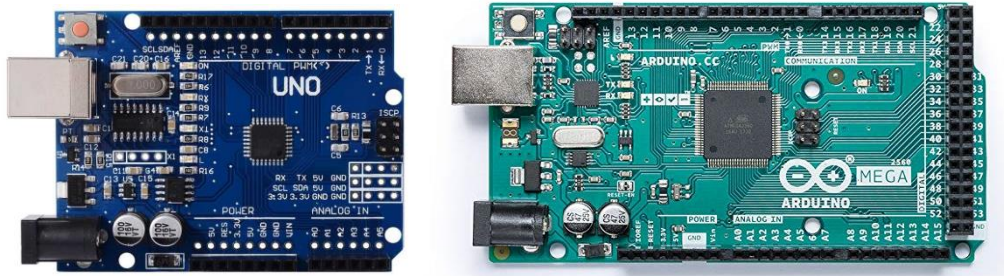


Fig 10. Arduino UNO (in left) and Arduino MEGA (in right) photos.

We have chosen to work with the Arduino MEGA2560 over Arduino UNO because this kind of boards is available for us. In addition, Arduino MEGA 2560 is a developer board based on ATmega2560 microcontroller. It is compatible with Arduino Duemilanove/UNO footprint. It means, the shields designed for Duemilanove will also fit to Mega board. However, there are some differences between functions of particular pins, thus not every shield can be used with Arduino MEGA. One could say, Arduino Mega is Arduino UNO’s older brother, bigger memory, more input/output pins, so it’s dedicated to more advanced applications than UNO. Totally it has 54 digital inputs/outputs (including 14 capable of PWM operation), 16 analog inputs, 4 serial ports (UART), SPI and I2C interfaces. Available memory is 256 KB of flash, 8 KB RAM and 4 KB EEPROM. The processor works with frequency of 16 MHz.

III. Arduino motor shield Rev3

The Arduino Motor Shield allows an easily control motor direction and speed using an Arduino. By simply address Arduino pins; it makes it very simple to incorporate a motor into a project. It also allows being able to power a motor with a separate power supply of up to 12v.

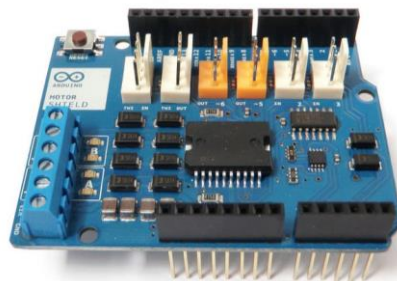


Fig 12. Arduino motor shield Rev3 photo.

The motor shield has two channels, which allows for the control of two DC motors, or 1 stepper motor.

Function	<u>Channel A</u>	<u>Channel B</u>
<i>Direction</i>	Digital 12	Digital 13
<i>Speed (PWM)</i>	Digital 3	Digital 11
<i>Brake</i>	Digital 9	Digital 8
<i>Current Sensing</i>	Analog 0	Analog 1

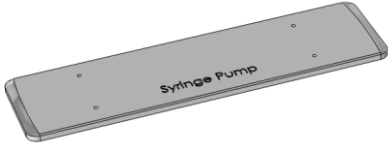
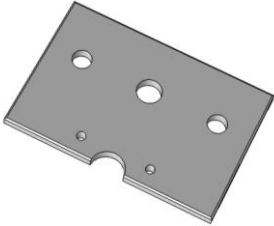
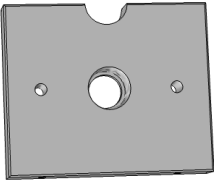
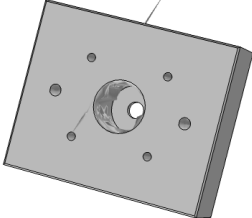
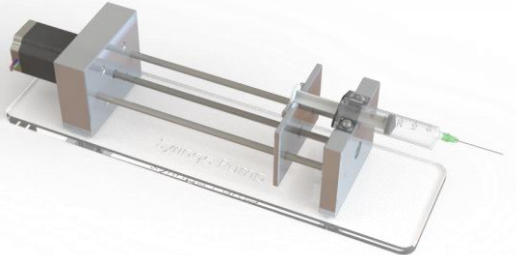
Fig 13. The pins breakdown.

Chapter 2. The syringe driver realization and their calibration.

With an external power supply, the motor shield can safely supply up to 12V and 2A per motor channel (or 4A to a single channel). There are pins on the Arduino that are always in use by the shield. By addressing these pins you can select a motor channel to initiate, specify the motor direction (polarity), set motor speed (PWM), stop and start the motor, and monitor the current absorption of each channel. The pins breakdown are shown in the figure 13.

IV. The hardware parts.

Using Comsol Multiphysics, we have designed the different parts used to realize the syringe driver aiming to print them with a 3D printer:

Designed parts	Specification
	The base
	The mobile part
	The fixed border 1
	The fixed border 2
	The final expected syringe driver

Tab1. The 3D printer design

Chapter 2. The syringe driver realization and their calibration.

Due to some circumstances, we were obliged to realize these prototypes by wood instead of PLA (by the 3D printer) in order to accelerate the realization and to gain in the total price of the project. On the other hand, the metal mechanical parts consist of the following elements:

	Trapezoidal screw
	Trapezoidal nut
	Linear shafts
	Bearings

Tab2. The metal mechanical parts.

The linear motion is made by the screw and the nut, which are connected to the motor shaft. The choice of the Trapezoidal screw and its length is well studied; the distance between the teeth is the same distance between two volume marks of the syringe.

V. Stepper motor pm551-048-hp69.

This kind of motor is commonly used for several applications such as: printers/scanners, flow control valves, slot machine and sewing machine. In our case, this stepper motor is the best choice because it gives the opportunity to control the motor speed perfectly by doing the right calibration. Furthermore, it is the only available stepper motor in the electronic shop without a delivery. The references characteristics of the stepper motor pm551-048-hp69 are described in the following table.

Motor Size	PM55L-048	
Number of Steps per Rotation	48(7.5°/Step)	
Drive Method	2-2 PHASE	
Drive Circuit	UNIPOLAR CONST. VOLT.	BIPOLAR CHOPPER
Drive Voltage	24[V]	24[V]
Current/Phase		800[mA]
Coil Resistance/Phase	30[Ω]	5.5[Ω]
Drive IC	2SC3346	UDN2916B-V
Magnet Material	Ferrite plastic magnet (MSPL) Polar anisotropy ferrite sintered magnet (MS50) Nd-Fe-B bonded magnet (MS70)	
Insulation Resistance	100M[Ω] MIN	
Dielectric Strength	AC 500[V] 1[min]	
Class of Insulation	CLASS E	
Operating Temp	-10[°C] ~ 50[°C]	
Storage Temp	-30[°C] ~ 80[°C]	
Operating Hum.	20[%] RH ~ 90[%] RH	

Tab3. The motor data sheet.

VI. Calibration of the syringe-driver.

One of the most important tasks is that the syringe driver has to be calibrated. We must take in consideration the following points: the rotation of the stepper motor, the length of the Trapezoidal screw and the dimensions of the syringe. The calibration can be generated so far by the Arduino code. We have to calculate the distance relative to one rotation, we have found that :

$$48 \text{ steps by rotation} \rightarrow 8\text{mm}$$

$$1 \text{ step} \rightarrow 0.16667 \text{ mm}$$

After that, we add this equation to the Arduino code, it will give an exact motion relative to the syringe volume calibration.

VII. LCD display and Keypad.

After we have designed and calibrated the syringe driver, we need its easiest usage. For that purpose, a keypad and an LCD display is used to control the syringe driver.

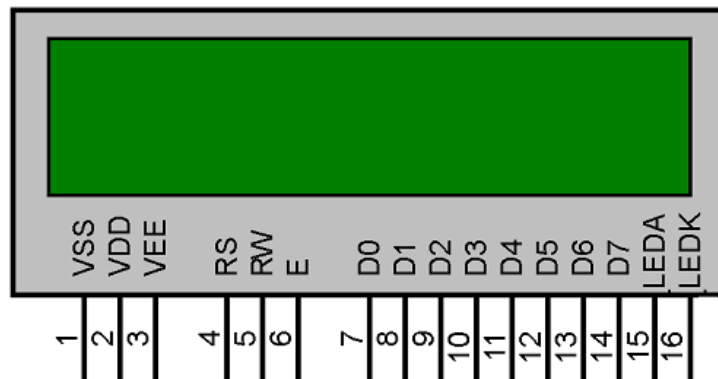


Fig 17. LCD display pins.

A liquid-crystal display (LCD) is a flat-panel display that uses the light-modulating properties of liquid crystals. LCDs are available to display arbitrary images (as in a general-purpose computer display) or fixed images with low information content, which can be displayed or hidden, such as preset words, digits, and seven-segment displays. Since LCD screens do not use phosphors, they rarely suffer image burn-in when a static image is displayed on a screen for a long time and its low electrical power consumption enables it to be used in battery-powered electronic equipment. In the following table, we describe each pin of the LCD display

Pin no.	Symbol	External connection	Function
1	V _{SS}	Power supply	Signal ground for LCM
2	V _{DD}		Power supply for logic for LCM
3	V ₀		Contrast adjust
4	RS	MPU	Register select signal
5	R/W	MPU	Read/write select signal
6	E	MPU	Operation (data read/write) enable signal
7~10	DB0~DB3	MPU	Four low order bi-directional three-state data bus lines. Used for data transfer between the MPU and the LCM. These four are not used during 4-bit operation.
11~14	DB4~DB7	MPU	Four high order bi-directional three-state data bus lines. Used for data transfer between the MPU
15	LED+	LED BKL power supply	Power supply for BKL
16	LED-		Power supply for BKL

Tab4. LCD display pin's signification.

On the other hand, a keypad is a set of buttons arranged in a block or "pad" which bear digits, symbols or alphabetical letters, it is commonly used in the Arduino world.

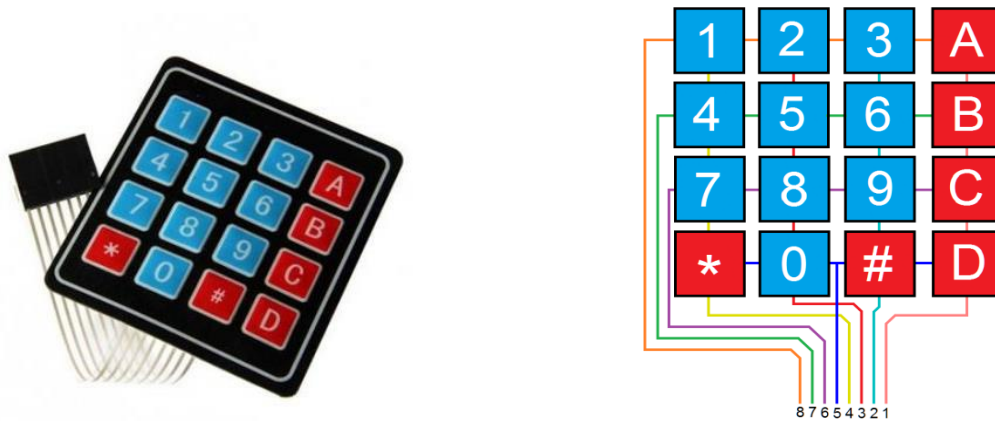


Fig 19. Keypad connections.

Inside the keypad there is a matrix of 4×4 (4 lines, 4 columns), the matrix keypads use a combination of four rows and four columns to provide button states to the host device, typically a microcontroller. Underneath each key is a pushbutton, with one end connected to one row, and the other end connected to one column.

And this is the final syringe driver shown in the following figure .

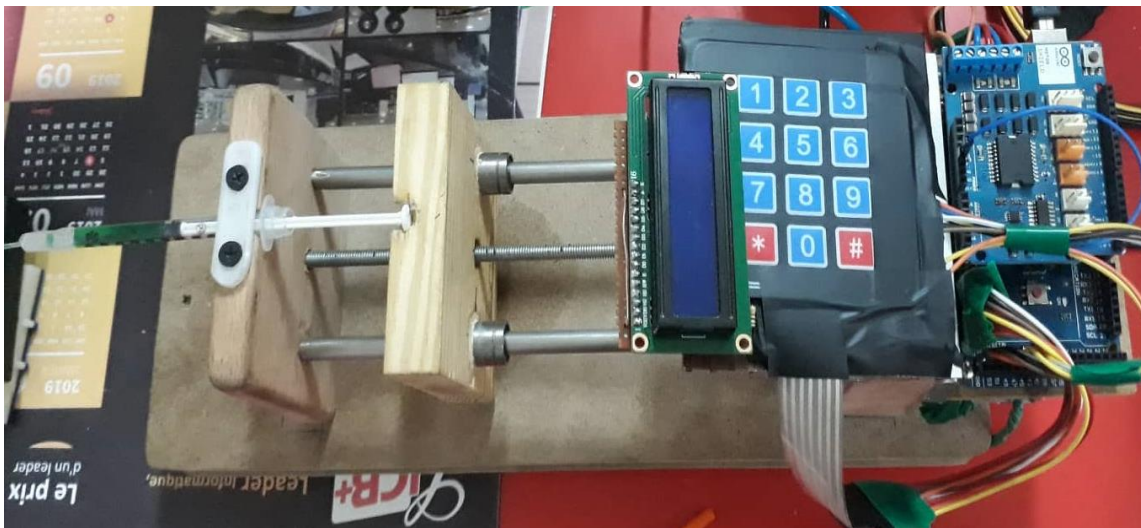


Fig 20.Final syringe driver

VIII. Test bed with an Optical mounting.

1. The flow-rate measurement.

We aim by this mounting to present a method to calculate the flow rate and the differential pressure. This mounting is based on the usage of the Optical Microscope that exists in our laboratory. The Microscope has the ability to record videos and photos, and this will help us to have several measurements of the Time that the fluid will make to cross the real distance.



Fig21. The digital microscope (PARALUX).

The Microscope gives us an amazing watch of the fluid's movement, we see in the following figure the displacement that we want to calculate

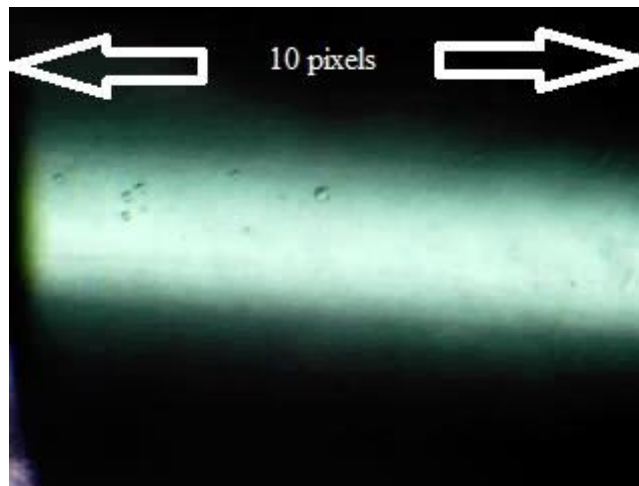


Fig22. The fluid's displacement under microscope.

Unfortunately, this Microscope has not a micro-ruler to determine the distance and the size of the object. Thus, we tried to order a micro-ruler called "the mire ruler", but due to some circumstances, we did not receive it. Then, we used the pixel number to know the distance that the fluid can make in order to calculate the flow rate, by using Microscope's photo. To convert pixels to millimeter, we use MATLAB program to determine the pixel number:

```
clear all;
clc;
close all;
im = 'fluid2.jpg'
imshow(im)
im1=im(1,:)
TotalPix = numel(im1)
size(im1)
```

Chapter 2. The syringe driver realization and their calibration.

This program gives us the exact pixel number in one line of a photo, and this will help us to know the distance of the line. Next, we convert the pixel number to millimeter using this table:

Pixel (X)	Millimeter [mm]
0.01 pixel (X)	0.0026458333 mm
0.1 pixel (X)	0.0264583333 mm
1 pixel (X)	0.2645833333 mm

Fig 23. Pixel/mm conversion.

After calculating the distance, we need to know the relative time that the fluid would make according to that distance. For that purpose, we effect several measurements using the recorded video, and after that; we take the average of the time measurements in order to reduce manipulating errors. Once we have the time and the distance, we can reach to the speed or the fluid's velocity using the relation:

$$V = \frac{D}{t} \dots\dots(5)$$

Where, v is the velocity, D is the distance and t is the related time.

Now we can easily calculate the flow rate by multiplying the velocity to the tube's section:

$$Q = V \cdot A \dots\dots(6)$$

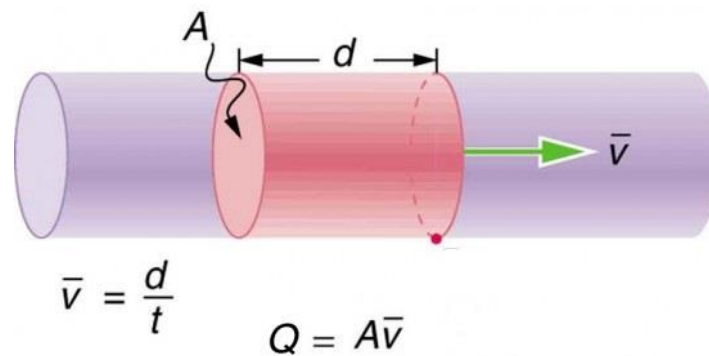


Fig 24. The schematic description of flow-rate equation.

In our case, the diameter of the tube is “ $d=1\text{mm}$ ”, Thus the section A would be:

$$A = \pi \times \frac{d^2}{4} \dots\dots(7)$$

By calculating the flow rate, we can get easily the differential pressure by using the Optical Microscope, since our fluid meets the Poiseuille law criteria. Where fluid is considered incompressible, newtonian fluid in a laminar flow.

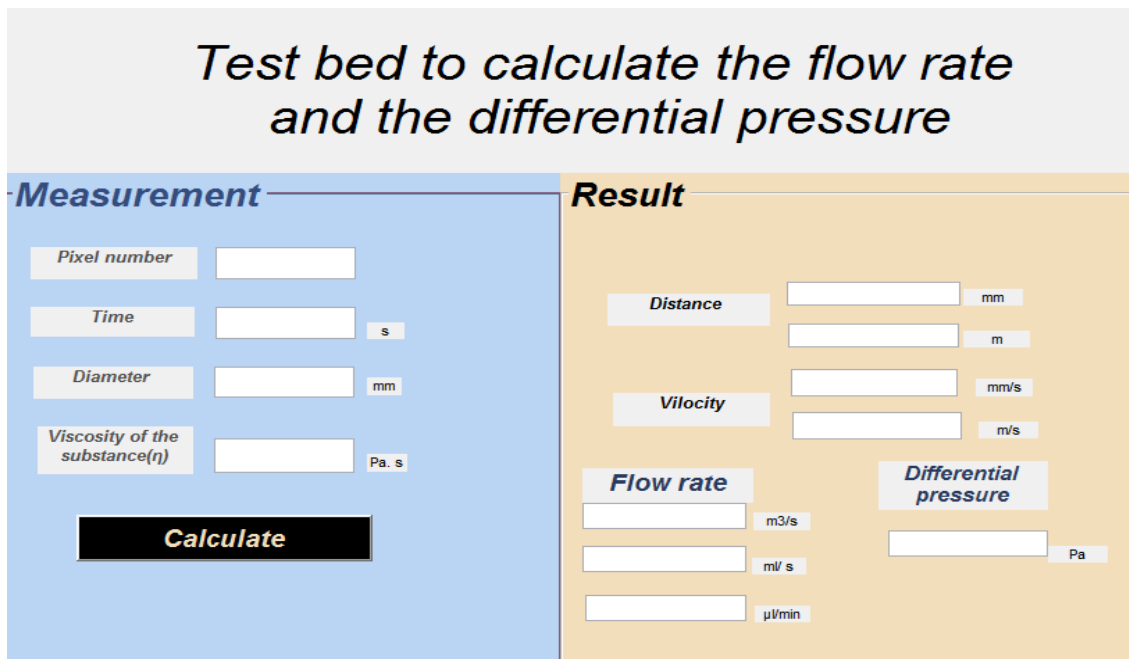


Fig25. The test-bed interface.

In order to facilitate the calculation, we design an interface using MATLAB as it is shown in the figure 24.

2. The flow-rate calibration.

We have calibrated the mechanism of the syringe driver. Where, we aim to find a validated flow-rate in order to inject it to the testing structures. For that purpose, we will use the optical mounting method for measuring the flow-rate. The variable data that we have are:

- ✓ the section of the tube “S”,
- ✓ the time between two respective steps “T1” of the motor (we control it through the Arduino code),
- ✓ the distance or the fluid course “D” ,
- ✓ and its relative time (the time that the fluid makes to travel the distance D) “T2”.

As it is shown in the lower figure, we fix some data such as: the distance D, the section of the tube “S” and and we leave time T1 as variable. We got the following measurement table.

Motor speed [mm/s]	TIME [s] ± 0.03 s	Flow-rate [ul/min]
0.8	0.33	377.824
0.6	0.98	127.226
0.5	1.05	118.745
0.47	1.24	100.55
0.37	1.38	90.3492
0.33	1.5	83.1213
0.3	1.57	79.4153
0.28	1.63	76.492
0.25	2.75	45.3389
0.23	3.98	31.3271

Tab5. The experimental measurements.

Chapter 2. The syringe driver realization and their calibration.

Observing the curve of the measurement Flow-rate as function as the motor speed, we find several linear fits; we will choose one interval that helps us. We can replace the motor speed by the flow-rate afterwards by changing the Arduino code in order to manipulate the flow-rate directly on the LCD display.

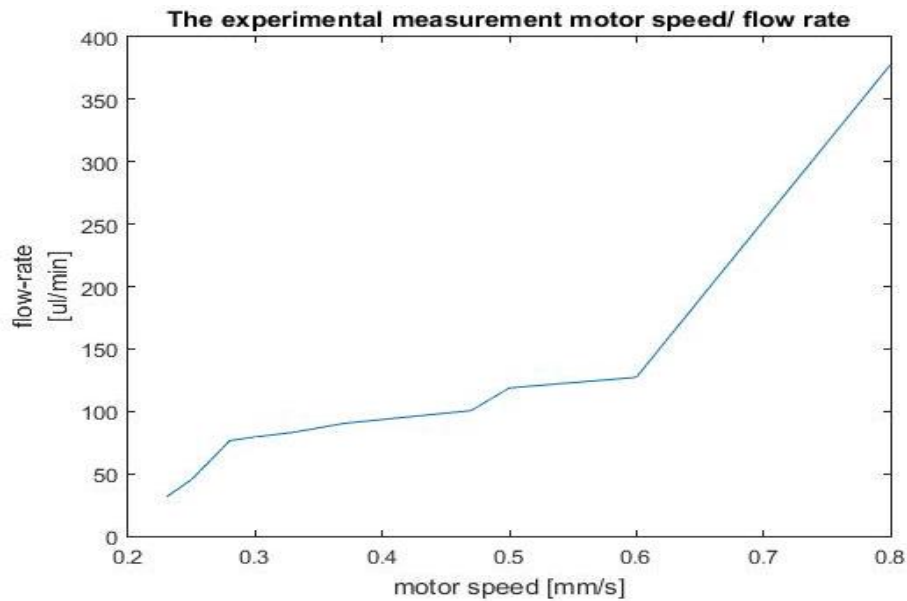


Fig 26. The linear flow-rate as function as motor speed.

Here, we can say that the validated interval would be [100 , 400] $\mu\text{l}/\text{min}$. Now, we will choose one value and use another method to verify it. In order to calculate the flow-rate, we will weigh the quantity of the fluid coming out from the syringe driver and divide it by time. We use a balance offsetting at 0g with the pot, after that, we set 100 $\mu\text{l}/\text{min}$ flow rate. Waiting for all the fluid go out, we measure the relative time. We find that the fluid weighs 0.44g and the relative time 3.92 min. Thus, the flow rate is 112 $\mu\text{l}/\text{min}$. Comparing it with the injected flow-rate, we can say that we are circling around the same value even though the error is little bit acceptable.

IX. Conclusion.

We have outlined on this chapter, the syringe driver realization the optical method that we have used to measure the flow-rate. Afterwards, we describe the flow-rate calibration of the syringe driver. The syringe driver will be used to inject a known flow-rate on the structures that we hope testing. Our syringe driver will deliver flow rates between 100 and 400 $\mu\text{l}/\text{min}$. we can also validate the other intervals but we should work on the Arduino code .

Chapter 3

Flow-rates measurements in valves micro-pumps

I. Introduction.

In the previous chapter, we have detailed the realization of the syringe driver and its calibration for the flow-rate delivery by using capillary channel. In this chapter, we will outline the testing valves structures designed for micro-pumps drug delivery. Firstly, we will try to test and measure the flow-rate relative of the two kind of passive structures called diffuser and nozzle elements. As well as, we will as well try to detail both structures and the key characteristics of each one of them. The most important is testing the enhanced structures of the diffuser/nozzle, this new design is the focusing PhD work of Mr Ahmed Slami who created this improved structure and tests it using COMSOL MULTIPHYSICS. In this chapter, we will try also to measure and compare experimentally the flow-rate for two different designs of micro-pumps valves. For this, we use soft lithography to fabricate the microfluidic valves design connected by Teflon flexible capillary. Where, 3D printer is used to fabricate the master mold with using ABS material.

II. Diffuser/ nozzle structure

Micro-pumps had received significant attention in medical and biological applications such as lab-on-a-chip, electronic cooling and biochemistry [7]. Generally, micro-valves are employed in the micro-pumps to achieve a higher efficiency. In practice, two different micro-valve structures have been widely used in the design of micro-pumps, including active valve [8], and valve-less structure [9]. The active valves are often using actuators structures. The design features easier flow controllability over a wide range of operating conditions at the expense of larger size and additional power consumption. To tackle this problem, the novel concept of a valve-less diffuser pump was first proposed by Van De Pol [10]. Stemme and Stemme [11] later took the concept a step forward with a workable and practical micro-pump. These no moving elements is used to accelerate the flow. In our case, we will use this structure in valvless micro-pumps which are composed of a diffuser/nozzle structure and a pumping chamber (figure).

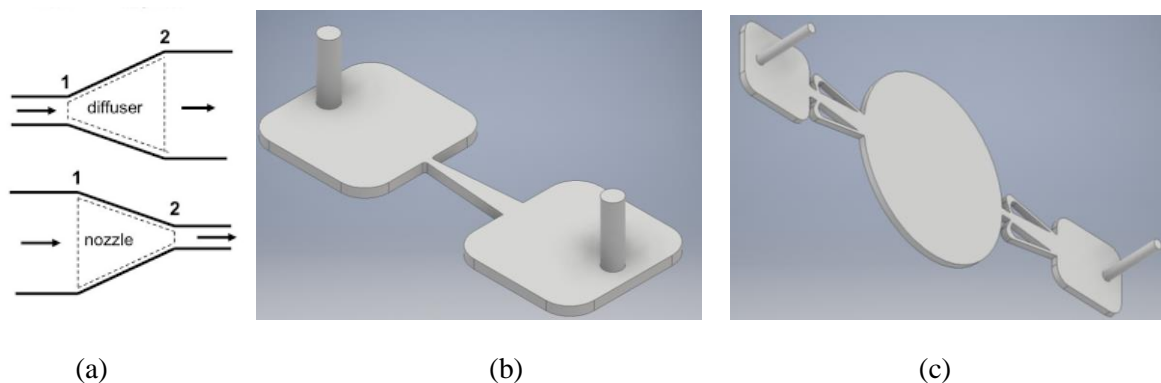


Fig 27. (a) Principle of diffuser nozzle. (b) The classic design of Diffuser/nozzle structure. (c) The ears design of Diffuser/nozzle structure.

In order to understand the mechanism of these structures, we can give the example of a diode. A diode is an electronic device which has two terminals and gives the opportunity of making the current flows in one direction. The same phenomena happens with the diffuser/nozzle structure, it has a positive and negative direction (direct / indirect flowing), we would have a small quantity of the fluid reversed on the indirect side (the backflow) represented by D_2 (flow-rate). In the positive direction (nozzle side), the nozzle design accelerates the fluid. This process gives acceleration in the velocity of fluid with decreasing pressure. Thus, the flow-rate in “2” is superior to flow-rate in “1” $\rightarrow (D_2 > D_1)$. In the diffuser structure, the opposite

mechanism happens; the fluid will be slowed down, the velocity decreases with an increasing in the pressure ($D_2 < D_1$). Our work will be mainly based on the verification of the diffuser/ nozzle structures by measuring the flow-rate in both inlet and the outlet respectively.

III. Enhanced diffuser/nozzle structure.

This new structure called ears diffuser/nozzle; is mainly designed to enhance the amount of the flow-rate as well as to decrease the backflow. The new structure is represented in the following figure

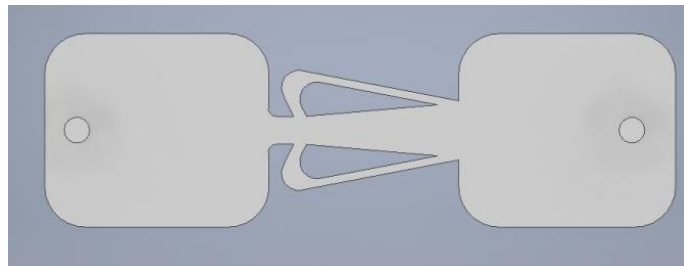


Fig 28. The design of the ears diffuser/nozzle.

Using COMSOL Multiphysics, recently Slami et al. [12] make a comparison between the ordinary diffuser/nozzle structure and ears diffuser/nozzle structures. The ears diffuser/nozzle structures give a satisfied improvement about 18% of the flow-rate in the direct side. Also, a remarkable decrease in the backflow is observed.

IV. Microfluidic structure realization

The PDMS is a polymer widely used in microfluidics to make devices such as lab on chip. Many laboratories use PDMS lithography replication also called soft lithography process. Soft lithography can be viewed as a complementary extension of photolithography. Originally, standard photolithography was mainly developed to deal with semiconductors used in the microelectronics industry. Photolithography is inherently well adapted to process photoresists. Thereby, most microfluidic structures still rely for fabricating polymer masters or mold.

IV.1 PDMS preparation

The PDMS (Polydimethylsiloxane) belongs to polymeric organosilicon family, it is widely used specially in the fluidic medical fields because of its bio-compatible and flexible features. In our work, the PDMS will be used to make these structures (diffuser/nozzle and ears diffuser/nozzle). The PDMS 182 kit from Sylgard [] is used The PDMS preparation can be divided into four main steps:

1. The scaling and mixing of the PDMS and the curing agent
2. The degassing to remove bubbles
3. The PDMS pouring on the mold
4. The PDMS baking

The prepared of mixed solution PDMS must be poured on the polymer master here we use the 3D printed negative mold. We use a vacuum round to degas and remove air bubbles. After that, the PDMS will be solidified by baking.

IV.2. Masters of molds fabrication

Using the 3D printer in the GBM laboratory called “Printrbot metal plus”, we have made the negative mold in PLA (Polylactic acid), This thermoplastic aliphatic polyester is largely utilized in the 3D printing. We have chosen the PLA because of its cheapness, its sensitivity and of course its existence in the market. In the following figure, we show an example of the master mold of the ears diffuser/nozzle.



Fig30. The negative mold of ears diffuser/nozzle structure.

The master mold method for making compact microfluidic structures in one step is impossible but requires two steps with using a bonding step. [10] developed a novel method to integrate the structure inside the PDMS structure in one step without using the bonding step. The method consists to use the ABS 3D printer wire and the acetone solution to create an interaction between the two by etching the ABS completely. As a definition, an ABS or “acrylonitrile butadiene styrene” is used by the 3D printers, it is a low cost material, and supports high temperature. In our case, we have found that there is an interaction ABS/ Acetone. The process of the method is the following:

1. We design the diffuser/nozzle and the enhanced structure itself without searching for its negative structure. Once the printing process is finished, we put it in a pot in such a way that the structure would be higher than the pot’s base.
2. We use the same PDMS preparation method as described.
3. Once the PDMS structure is solidified, we use the acetone solution to absorb all the ABS designed structure and we let the interaction for one or two days.
4. We wash the structure with distilled water and here is the diffuser/nozzle structure printed inside the PDMS.

We have to be extremely careful while dealing with the acetone solution, using the chemical’s material manipulation (gloves, glasses, laboratory apron...), because it may cause harmful eye’s injuries and skin inflammation. The printed structures are shown in figure below.

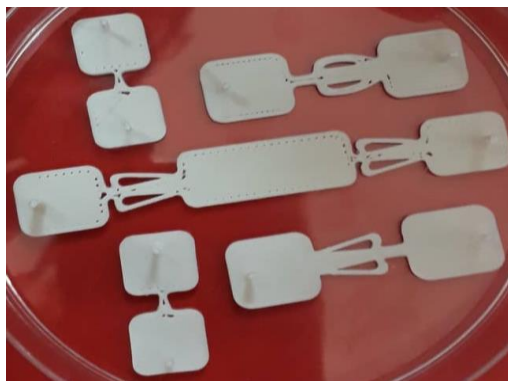


Fig 31. The 3D printed ABS structures.

The PDMS is poured on the microstructures; it is cross-linked to become solid. After that, we used acetone to react with the ABS structure. Unfortunately, the only successful structure is the simple diffuser / nozzle because of the difficulty we face is the extraction of ABS reacted from the structure. To do this, our test will focus on the simple diffuser / nozzle structure; the operation will be described below.

IV. Test protocol of micro-valves.

Generally, micro-pump is composed of a pumping chamber with diffuser/nozzle elements as an inlet and an outlet. Above the pumping chamber, we are aiming to put an actuator membrane such as a piezoelectric element. If the membrane of the chamber deforms outward, more liquid circulates from the inlet than the outlet. On the other hand, if the membrane deforms inward, more the liquid goes to the outlet than the inlet. The mechanism of the system is shown in the following figure.

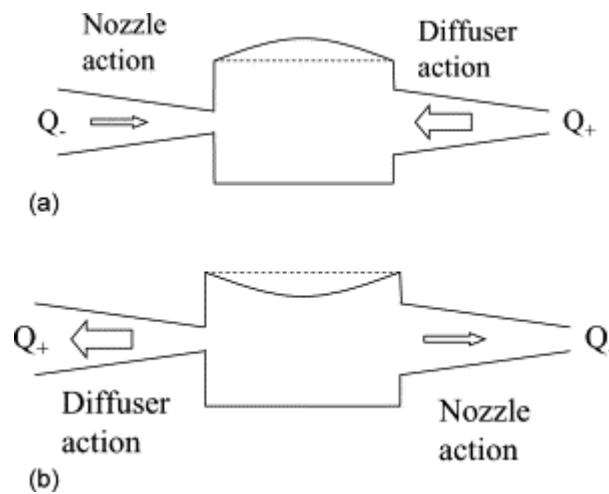


Fig 32. Micro-pump mechanism

To validate the effectiveness of micro-valves, we can use the syringe driver whose realization is described in chapter 2. In this case, we don't need a complete micro-pump to test these structures. For the diffuser side, using the syringe driver with a known flow-rate $D1$ we inject a known pressure in the inlet. In the outlet side, we use the microscope in order to determine the time of displacement and then knowing the flow-rate $D2$. Then we calculate the difference $D2-D1$.

If $D2-D1 > 0$ → we are talking about the diffuser side or the positive side.

If $D2-D1 < 0$ → we are talking about the nozzle side or the negative side.



Fig 33.Testing the simple diffuser/nozzle structure.

In order to determine the time of displacement and minimizing the error, we have done several calculation through the chronometer and then we took the average. The results are shown in the following table.

The structure	The time of displacement [s]	D1 [$\mu\text{l}/\text{min}$]	D2 [$\mu\text{l}/\text{min}$]
The diffuser side	0.544	100	229.195
The nozzle side	1.48	100	80

Tab 5. The result table.

The measurement in the diffuser side or the positive side, D2 increase clearly in comparison with D1. However, the measurement in the nozzle side or the negative side D2 decrease in comparison with D1. These results are logical for the use of this type of valve in micropumps with a gain greater than 200% in the diffuser direction and losses of 20% in the nozzle direction. Thanks to these results, we can validate that structure with its dimension. As perspective, we will play afterwards on the dimensions in order to reduce more and more as well as we will test the ears diffuser nozzle structure.

V. Conclusion.

In this chapter, we describe the diffuser/nozzle elements, the proprieties of each of the structure, as well as, the whole predicted micro-pumps. Also, we details method of fabrication of micro-valves structure. The syringe driver was used to validate the effectiveness of micro-valves. The final goal of the micro-pump is delivering the insulin continuously and automatically. As perspectives, we will try to repeat the PDMS operation to test the other structures with different dimensions; in addition, the most important thing is to test the whole micro-pump. Also, we should confront experimentally study to finite element modeling to optimize the micro-pumps design.

Conclusion.

In this project, we will be interested on the flow-rate measurements in microfluidic devices by using Poiseuille's law with an optical microscope. Where, we developed a test bench that allows us to test different kinds of micro-pump and/or micro-valves for rapid drug delivery designed in Biomedical Engineering laboratory. Firstly, we have made a syringe driver that allows delivering a continuous micro-flow. The fabricated syringe driver coupled with the optical microscope allows us to measure the flow-rate. We use measurements by displacement of a meniscus method to measure fluid flows in microfluidic structures. To facilitate measurement, we design an interface using MATLAB for digital control.

In this study, we describe the flow-rate calibration of the syringe driver. The syringe driver will be used to inject a known flow-rate on the structures that we hope testing. Our syringe driver will deliver flow rates between 100 and 400 $\mu\text{l}/\text{min}$. Here, we test a classical diffuser/nozzle element. we have realized the diffuser/nozzle structures made of PDMS, we have tested and validated one succeeded structure.

In this study, we details method of fabrication of micro-valves structure. The syringe driver was used to validate the effectiveness of micro-valves. As perspectives, we will try to fabricate other structures with different dimensions, as well as, the most important thing is to test the whole micro-pump. Also, we should confront experimentally study to finite element modeling to optimize the micro-pumps design.

References

1. LEFEVRE, R. Conception et realization d'une micropompe intelligente: applications dans le domaine biomedical. PhD thesis 2014.
2. ANDUZE, M. etude experementale et numerique de microecoulements liquides dans les microsystems fluidiques. PhD thesis 2000.
3. URBANEK W. (1994) - " An investigation of the temperature dependence of Poiseuille numbers in microchannel flow", *Thesis*, University of Pennsylvania.
4. ACERO M. C., PLAZA J. A., ESTEVE J., CARMONA M., MARCO S. and SAMITIER J. (1997) - "Design of a modular micropump based on anodic bonding", *Journal of Micromechanics and Microengineering*, vol. 7, pp. 179-182.
5. SCHNELL G. (1997) - "Measurement of very small liquid flows", *Experimental Thermal and Fluid Science*, vol. 15, pp. 406-412.
6. AMEEL T. A., WARRINGTON R. O., WEGENG R. S. and DROST M. K. Miniaturisation technologies applied to energy systems", (1997).
7. D. J. Laser et J. G. Santiago, « A review of micropumps », *J. Micromechanics Microengineering*, vol. 14, n° 6, p. R35-R64, juin 2004.
8. F. Meshkinfam et G. Rizvi, « Design and Simulation of MEMS Based Piezoelectric Insulin Micro-Pump », p. 6, 2015
9. S. Singh, N. Kumar, D. George, et A. K. Sen, « Analytical modeling, simulations and experimental studies of a PZT actuated planar valveless PDMS micropump », *Sens. Actuators Phys.*, vol. 225, p. 81-94, avr. 2015.
10. van de pol F C M, van Lintel HTG, Elwenspoek M and Fluitman J H J 1990 A thermopneumatic micropump based on micro-engineering techniques *Sensors Actuators A* **21** 198_ 202.
11. E. Stemme et G. Stemme, « A valveless diffuser/nozzle-based fluid pump », *Sens. Actuators Phys.*, vol. 39, n° 2, p. 159-167, 1993.
12. A. Slami and al. « To fluidic Diode for Biomedical Application». COMSOL Conference in Lausanne, 2018.

Annexe

- The Arduino code.

```
#include <LiquidCrystal.h>

#include <Keypad.h>

const byte LIGNES = 4;

const byte COLONNES = 4;

const int RS=44;//8;

const int E=42;//9;

const int D4=52;//10;

const int D5=50;//11;

const int D6=48;//12;

const int D7=46;//13;

char touches[LIGNES][COLONNES] = {

  {'1','2','3','A'},

  {'4','5','6','B'},

  {'7','8','9','C'},

  {'*','0','#','D'}

};

byte BrochesLignes[LIGNES] = { A11, A10, A9,A8};

byte BrochesColonnes[COLONNES] = { A15,A14,A13,A12 };
```

```
char touche;

int t_,q_;

LiquidCrystal lcd(RS, E, D4, D5, D6, D7);

Keypad clavier = Keypad( makeKeymap(touches), BrochesLignes, BrochesColonnes, LIGNES,
COLONNES );

void setup() {

pinMode(22, OUTPUT);

lcd.begin(16,2);

delay(10);

t_=3;

q_=10;

lcd.print(" **WELCOME**" );

lcd.setCursor(0,1);

delay(2000);

lcd.clear();

lcd.print(" Please Press:");

lcd.setCursor(0,1);

delay(3000);
```

```
lcd.clear();

lcd.clear();

lcd.blink();

//lcd.setCursor(0,1);

//delay(6000);

lcd.clear();

lcd.print("1:BACKWARD *:PARA");

lcd.setCursor(0,1);

lcd.print("2:FORWARD");

lcd.setCursor(12,2);

//establish motor direction toggle pins

pinMode(12, OUTPUT); //CH A -- HIGH = forwards and LOW = backwards???

pinMode(13, OUTPUT); //CH B -- HIGH = forwards and LOW = backwards???

pinMode(9, OUTPUT); //brake (disable) CH A

pinMode(8, OUTPUT); //brake (disable) CH B}

void back (int n , int delaylength){

char tt='k';

int i;

n=n/0.16667;

for(i=1;i<=n;i++){
```



```
lcd.clear();

lcd.setCursor(0,1); lcd.print("*: PAUSE #:STOP");

lcd.setCursor(0,0);lcd.print("Forward "); lcd.print(i);lcd.print("/");lcd.print(n);

tt = clavier.getKey();

if (tt == '*'){lcd.setCursor(0,1); lcd.print("*: PLAY #:STOP"); tt='k'; while ((tt != '*')&&(tt != '#'))tt
= clavier.getKey();}

if (tt == '#') i=n+1;

tt='k';

digitalWrite(9, LOW); //ENABLE CH A

digitalWrite(8, HIGH); //DISABLE CH B

digitalWrite(12, HIGH); //Sets direction of CH A

analogWrite(3, 255); //Moves CH A

delay(delaylength);

digitalWrite(9, HIGH); //DISABLE CH A

digitalWrite(8, LOW); //ENABLE CH B

digitalWrite(13, LOW); //Sets direction of CH B

analogWrite(11, 255); //Moves CH B

delay(delaylength);

digitalWrite(9, LOW); //ENABLE CH A

digitalWrite(8, HIGH); //DISABLE CH B
```

```

digitalWrite(12, LOW); //Sets direction of CH A

analogWrite(3, 255); //Moves CH A

delay(delaylength);

digitalWrite(9, HIGH); //DISABLE CH A

digitalWrite(8, LOW); //ENABLE CH B

digitalWrite(13, HIGH); //Sets direction of CH B

analogWrite(11, 255); //Moves CH B

delay(delaylength); } }

void forward (int n , int delaylength){

int i;

n=n/0.16667;

char tt='k';

for(i=1;i<=n;i++){

lcd.clear();

lcd.setCursor(0,1); lcd.print("*: PAUSE #:STOP");

lcd.setCursor(0,0);lcd.print("Backward "); lcd.print(i);lcd.print("/");lcd.print(n);

tt = clavier.getKey();

if (tt == '*'){lcd.setCursor(0,1); lcd.print("*: PLAY #:STOP"); tt='k'; while ((tt != '*')&&(tt != '#'))tt = clavier.getKey();}

if (tt == '#') i=n+1;

```

```
tt='k';

digitalWrite(9, LOW); //ENABLE CH A

digitalWrite(8, HIGH); //DISABLE CH B

digitalWrite(12, HIGH); //Sets direction of CH A

analogWrite(3, 255); //Moves CH A

delay(delaylength);

digitalWrite(9, HIGH); //DISABLE CH A

digitalWrite(8, LOW); //ENABLE CH B

digitalWrite(13, HIGH); //Sets direction of CH B

analogWrite(11, 255); //Moves CH B

delay(delaylength);

digitalWrite(9, LOW); //ENABLE CH A

digitalWrite(8, HIGH); //DISABLE CH B

digitalWrite(12, LOW); //Sets direction of CH A

analogWrite(3, 255); //Moves CH A

delay(delaylength);

digitalWrite(9, HIGH); //DISABLE CH A

digitalWrite(8, LOW); //ENABLE CH B

digitalWrite(13, LOW); //Sets direction of CH B

analogWrite(11, 255); //Moves CH B
```

```
delay(delaylength);} }
```

```
int f(char r){
```

```
    if(r=='0') return 0 ;
```

```
else if(r=='1') return 1 ;
```

```
else if(r=='2') return 2 ;
```

```
else if(r=='3') return 3 ;
```

```
else if(r=='4') return 4 ;
```

```
else if(r=='5') return 5 ;
```

```
else if(r=='6') return 6 ;
```

```
else if(r=='7') return 7 ;
```

```
else if(r=='8') return 8 ;
```

```
else if(r=='9') return 9 ;
```

```
else return -1; }
```

```
int f1(){
```

```
int y=0;
```

```
char tt;
```

```
while(1==1){
```

```
tt = clavier.getKey();
```

```
while (tt == NO_KEY)tt = clavier.getKey();
```

```
if(tt=='*')return y;
```

```

else if(f(tt)!=-1){y=y*10+f(tt);lcd.print(tt);tt='K';}}

return y; }

void loop(){

  digitalWrite(22, LOW);

  touche = clavier.getKey();

  if (touche != NO_KEY){

    if (touche=='1')  { lcd.clear(); lcd.print("BACKWARD MOTION");
forward(q_,t_);touche=='K'; delay (200); }

    else if (touche=='2')  { lcd.clear(); lcd.print("FORWARD MOTION");
back(q_,t_);touche=='K'; delay (200); }

    else if (touche=='*')  { lcd.clear(); lcd.print("Flow90_120ul/min *: NEXT");lcd.setCursor(0,1);
t_=173.5-(0.16*f1()); lcd.clear(); lcd.print("VOLUME *: NEXT");lcd.setCursor(0,1); q_=f1();
touche=='K'; }

  lcd.clear();

  lcd.clear();

  lcd.print("1:BACKWARD *:PARA");

  lcd.setCursor(0,1);

  lcd.print("2:FORWARD");

  lcd.setCursor(12,2);}}

```